Available online at www.sciencedirect.com
SCIENCE DIRECT®
Biomaterials 26 (2005) 1337–1348
Biomaterials
www.elsevier.com/locate/biomaterials

Fast setting calcium phosphate–chitosan scaffold: mechanical properties and biocompatibility ☆

Hockin H.K. Xu[a,*], Carl G. Simon Jr[b]

[a] *Paffenbarger Research Center, American Dental Association Foundation, USA*
[b] *National Institute of Standards and Technology, Gaithersburg, MD 20899-8546, USA*

Received 9 March 2004; accepted 30 April 2004

Abstract

Calcium phosphate cement (CPC) sets in situ to form hydroxyapatite and is highly promising for a wide range of clinical applications. However, its low strength limits its use to only non-stress applications, and its lack of macroporosity hinders cell infiltration, bone ingrowth and implant fixation. The aim of this study was to develop strong and macroporous CPC scaffolds by incorporating chitosan and water-soluble mannitol, and to examine the biocompatibility of the new graft with an osteoblast cell line and an enzymatic assay. Two-way ANOVA identified significant effects on mechanical properties from chitosan reinforcement and powder:liquid ratio ($p<0.001$). The flexural strength of CPC–chitosan composite at a powder:liquid ratio of 2 was (13.6 ± 1.2) MPa, which was significantly higher than (3.2 ± 0.6) MPa for CPC control without chitosan (Tukey's at 0.95). At a powder:liquid ratio of 3.5, CPC–chitosan had a strength of (25.3 ± 2.9) MPa, which was significantly higher than (10.4 ± 1.7) MPa for CPC control. The scaffolds possessed total pore volume fractions ranging from 42.0% to 80.0%, and macroporosity up to 65.5%. At total porosities of 52.2–75.2%, the scaffold had strength and elastic modulus values similar to those of sintered porous hydroxyapatite and cancellous bone. Osteoblast mouse cells (MC3T3-E1) were able to adhere, spread and proliferate on CPC–chitosan specimens. The cells, which ranged from about 20 to 50 μm including the cytoplasmic extensions, infiltrated into the 165–271 μm macropores of the scaffold. In summary, substantial reinforcement and macroporosity were imparted to a moldable, fast-setting, biocompatible, and resorbable hydroxyapatite graft. The highly porous scaffold may facilitate bone ingrowth and implant fixation in vivo. In addition, the two to three times increase in strength may help extend the use of CPC to larger repairs in moderately stress-bearing locations.

Keywords: Calcium phosphate scaffold; Hydroxyapatite; Chitosan; Strength; Bone tissue engineering; Biocompatibility

1. Introduction

Musculoskeletal conditions are becoming a major health concern because of an aging population and sports- and traffic-related injuries. More than 3 million musculoskeletal procedures were performed in 1988 in the United States alone, and this number is predicted to increase dramatically as the life expectancy of the world population increases [1]. Hydroxyapatite has found wide use due to its chemical and crystallographic similarity to the carbonated apatite in human bones and teeth [2,3]. While sintered hydroxyapatite can be machined and used in prefabricated forms, several formulations of calcium phosphate cements can be molded as pastes and harden in situ [4–14]. One calcium phosphate cement [4], referred to as CPC, is comprised of a mixture of fine particles of tetracalcium phosphate (TTCP: $Ca_4(PO_4)_2O$) and dicalcium phosphate anhydrous (DCPA: $CaHPO_4$). The CPC powder can be mixed with water to form a paste that can conform to osseous defects with complex shapes and set in vivo to form hydroxyapatite with excellent osteoconductivity [15–19]. CPC is highly promising for use in a number of craniofacial and orthopedic procedures, including the reconstruction of

☆ Official contribution of the National Institute of Standards and Technology; not subject to copyright in the United States.

*Corresponding author. National Institute of Standards and Technology, Gaithersburg, MD 20899-8546, USA. Tel.: +1-301-975-6804; fax: +1-301-963-9143.
E-mail address: hockin.xu@nist.gov (H.H.K. Xu).

0142-9612/$ - see front matter © 2004 Elsevier Ltd. All rights reserved.
doi:10.1016/j.biomaterials.2004.04.043

frontal sinus, augmentation of craniofacial skeletal defects, use in endodontics, and the repair of periodontal bone defects [4,15–19].

However, washout of the CPC paste can occur in vivo when it comes in contact with physiological fluids or when bleeding occurs due to the difficulty in some cases to achieve complete hemostasis [20]. While the earlier versions of the CPC paste took a relatively long time of >60 min to harden, the recently developed CPC–chitosan pastes [21,22] possessed a fast-setting ability of hardening in 6.7 min [23]. Fast setting was accompanied by the anti-washout characteristic, manifested by the freshly mixed CPC–chitosan paste exhibiting no dissolution when immersed in a physiological solution. In comparison, the conventional CPC paste showed significant dissolution and washout in the same solution [23].

The second challenge facing CPC is its relatively low strength and susceptibility to brittle fracture, which have limited the use of CPC to only non load-bearing applications [15–19]. The use of CPC was "limited to the reconstruction of non-stress-bearing bone" [16], and "clinical usage was limited by ... brittleness ..." [18]. Furthermore, the third problem with CPC is that it consists of only micropores with pore sizes of submicrometer to a few micrometers. Previous studies on hydroxyapatite implants have found that macropore sizes of about 100 μm to several hundred μm are required for bone ingrowth [24–31]. Macropores have been shown to be beneficial in facilitating cell infiltration and tissue ingrowth [32–36]. In a study on periodontal repair [37], most CPC implants were exfoliated prior to being integrated with the surrounding bone. Recovered implants showed that the material had set adequately and had converted to hydroxyapatite, and that the loss was due to mechanical displacement [37]. Recent studies built macropores into conventional CPC without chitosan to enhance tissue ingrowth and implant fixation [38]. However, it was found that "incorporating macropores into the cement has always led to a significant decrease in mechanical strength" [19], by as much as an order of magnitude [38,39].

Therefore, attempts were made to increase the strength of CPC while forming macropores. One study used water-soluble mannitol crystals as a porogen (or pore forming agent) in CPC together with aramid fibers to produce a macroporous yet strong CPC [39]. In a separate study [38], large-diameter resorbable fibers were incorporated into CPC to provide the implant with the needed early strength; after a few weeks, the fibers were dissolved producing long cylindrical pores in the CPC for bone ingrowth [40]. Besides using fibers, the incorporation of chitosan, a natural biopolymer, was also found to significantly increase the CPC strength and strain before failure [21]. However, no macropores were built into the CPC–chitosan composite in those studies [21,22]. Recently, both chitosan and an absorbable fiber mesh were incorporated into CPC to achieve a substantial synergistic reinforcement [41]; it took a relatively long time of 12 weeks to dissolve the meshes and create macropores in the CPC. In a more recent study, both chitosan and a quickly soluble mannitol porogen were incorporated into CPC to result in a tailored macropore formation rate to match the bone repair rate [23], but only a single mass fraction of mannitol was used and a single powder-to-liquid ratio was tested in that study. In addition, the biocompatibility and cell response of the CPC–chitosan composites had not been investigated.

In the present study, CPC–chitosan–mannitol scaffolds were developed with a series of powder-to-liquid ratios and a wide range of mannitol content. The rationale for the microstructural design was that the mannitol crystals would quickly dissolve upon contact with the physiological liquid in vivo to create macropores for bone ingrowth, while the chitosan would provide the needed strength for the implant. The effect of chitosan on mechanical properties was evaluated, and the composite mechanical properties were measured as a function of pore volume fraction up to 80% for the scaffold. The biocompatibility of the new composite was examined with an osteoblast cell line, and the cell viability was quantified using an enzymatic assay.

2. Materials and methods

2.1. Materials development

The TTCP powder was synthesized from a solid-state reaction between equimolar amounts of $CaHPO_4$ (dicalcium phosphate anhydrous, or DCPA) and $CaCO_3$ (Baker Analyzed Reagents, J. T. Baker Chemical, Phillipsburg, NJ), which were mixed and heated at 1500°C for 6 h in a furnace (Model 51333, Lindberg, Watertown, WI). The heated mixture was quenched to room temperature, ground in a ball mill (Retsch PM4, Brinkman, NY) and sieved to obtain TTCP particles with sizes ranging from approximately 1 to 80 μm, with a median particle size of 17 μm. The DCPA powder was ground for 24 h and sieved to obtain particles with sizes ranging from approximately 0.4 to 3 μm, with a median particle size of 1 μm. The TTCP and DCPA powders were then mixed in a micromill (Bel-Alert Products, Pequannock, NJ) in equimolar amounts to form the CPC powder.

Two groups of specimens were fabricated. The first group was made to examine the effects of chitosan reinforcement and powder:liquid ratio. Chitosan and its derivatives are natural biopolymers that are biocompatible, biodegradable and osteoconductive [10,21,23,42–44]. In the present study, chitosan lactate (referred

to as chitosan in this paper; technical grade, VANSON, Redmond, WA) was mixed with distilled water at a mass fraction of 15% to form the CPC liquid, because a previous study [21] showed that this mass fraction produced specimens with the highest strength. This liquid was then mixed with the CPC powder to make specimens. As shown in a previous study, the incorporation of chitosan imparted fast-setting to the CPC, reducing the paste hardening time from 69.5 to 6.7 min [23]. In the present study, CPC powder:liquid mass ratios of 2.0, 3.0, 3.25, 3.5, 3.75, 4.0, and 4.5 were selected because ratios higher than 4.5 yielded a paste that was too dry to mix and mold, and ratios less than 2.0 produced specimens with low strength. This constituted a 2×7 design with two levels of chitosan (0% or 15%) and seven levels of powder:liquid ratio. Each mixed paste was placed into stainless steel molds of 3 mm × 4 mm × 25 mm to make flexural specimens. The paste in each mold was sandwiched between two glass slides, and set in a humidor with 100% relative humidity at 37°C for 4 h. The hardened specimens were demolded and immersed in a simulated physiological solution (1.15 mmol/l Ca, 1.2 mmol/l P, 133 mmol/l NaCl, 50 mmol/l HEPES, buffered to a pH of 7.4) stored in an oven at 37°C for 20 h prior to testing [21].

The second group of specimens was fabricated to investigate the effect of mannitol content, and hence macropore volume fraction, on scaffold properties. A water-soluble porogen, mannitol, was used in CPC because mannitol has the appropriate solubility, is non-toxic, and is physiologically compatible [38,39]. Mannitol ($CH_2OH[CHOH]_4CH_2OH$, Sigma Chemical, St. Louis, MO) was recrystallized in an ethanol/water solution at 50/50 by volume, filtered, dried, ground, and sieved through openings of 500 μm (top sieve) and 300 μm (bottom sieve) [23]. The mannitol crystals thus obtained were mixed with the CPC powder to form eight different CPC–mannitol powders, at mannitol/(mannitol + CPC powder) mass fractions of 0%, 10%, 20%, 30%, 40%, 50%, 60%, and 70%, respectively. For each powder, a powder:liquid ratio of 3.5 was used because the results of the first group of specimens showed that this ratio yielded the highest strength. The CPC liquid containing 15% chitosan was used because the first group of specimens with 15% chitosan had significantly higher strength than the specimens with 0% chitosan. The paste was mixed, placed into molds in a humidor for 4 h, and then immersed in a physiological solution at 37°C for 20 h as described above. This immersion dissolved the mannitol and created macropores [39].

2.2. Mechanical testing and porosity measurement

A three-point flexural test with a span of 20 mm was used to fracture the specimens at a crosshead speed of 1 mm/min on a computer-controlled Universal Testing Machine (model 5500R, Instron Corp., Canton, MA) [45]. The test was conducted in air at a relative humidity of about 50%.

The halves from the flexural test of specimens in which the mannitol was dissolved were used to measure the density and porosity. The sides and ends of each specimen were polished with 600 SiC paper to render them flat and approximately parallel [39]. The specimens were dried in a vacuum oven (Model DP-21, American Scientific Products, McGaw Park, IL) at 60°C for 24 h. As in a previous study [39], the density of the materials was measured by using the specimen mass divided by the specimen volume. The volume was calculated by the specimen dimensions measured with a micrometer, with each linear dimension the average of three locations along the specimen. A previous study showed that this method yielded density that closely matched values measured by a mercury intrusion method [39]. Thus, six specimens were measured for each material.

CPC consists of intrinsic microporosity and additional macroporosity from mannitol dissolution. The total porosity, P_{total}, of the specimen can be obtained by

$$P_{\text{total}} = (d_{\text{HA}} - d_{\text{measured}})/d_{\text{HA}}, \quad (1)$$

where d_{HA} is the density of fully dense hydroxyapatite which is 3.14 g/cm^3 [37], and d_{measured} is the measured density at a specific mannitol mass fraction. As detailed in a previous study [39], the macropore volume fraction from mannitol dissolution, P_{mannitol}, can be obtained by

$$P_{\text{mannitol}} = 1 - d_{\text{measured}}/d_{\text{measured-0\%}}, \quad (2)$$

where d_{measured} is the measured density of specimen with a specific mannitol content, and $d_{\text{measured-0\%}}$ is the measured density of CPC with 0% mannitol [39].

2.3. Cell culture experiments

Because cell culture toxicity assays are the international standard for biocompatibility screening [46], in vitro cell culture was performed to evaluate the biocompatibility of the new cement formulation. MC3T3-E1 osteoblast-like cells (Riken, Hirosaka, Japan) were cultured following established protocols [46,47]. Cells were cultured in flasks at 37°C and 100% humidity with 5% CO_2 (volume fraction) in α modified Eagle's minimum essential medium (Biowhittaker, Walkersville, MD). The medium was supplemented with 10% volume fraction of fetal bovine serum (Gibco, Rockville, MD) and kanamycin sulfate (Sigma, St. Louis, MO), and changed twice weekly. The cultures were passaged with 2.5 g/l trypsin containing 1 mmol/l EDTA (Gibco, Rockville, MD) once per week. Cultures of 90% confluent cells were trypsinized, washed and suspended in fresh media. CPC without chitosan (CPC control) and CPC with 15% chitosan were tested, both at a powder:liquid ratio of 3.5. Fifty thousand cells

diluted into 2 ml of media were added to each well containing a specimen or to an empty well of tissue culture polystyrene (TCPS, as a biocompatible control), and incubated for 1 or 14 d (2 ml of fresh media every 2 d) [48,49].

After 1 or 14 d incubations of the cells on the CPC–chitosan, CPC control or TCPS control, the media was removed and the cells were washed two times in 2 ml of Tyrode's Hepes buffer (140 mmol/l NaCl, 0.34 mmol/l Na_2HPO_4, 2.9 mmol/l KCl, 10 mmol/l Hepes, 12 mmol/l $NaHCO_3$, 5 mmol/l glucose, pH 7.4). Cells were then stained and viewed by epifluorescence microscopy (Eclipse TE300, Nikon, Melville, NY). Staining of cells was done for 5 min with 2 ml of Tyrode's Hepes buffer containing 2 μmol/l calcein-AM and 2 μmol/l ethidium homodimer-1 (both from Molecular Probes, Eugene, OR). Calcein-AM is a nonfluorescent, cell-permeant fluorescein derivative, which is converted by cellular enzymes into cell-impermeant and highly fluorescent calcein. Calcein accumulates inside live cells having intact membranes causing them to fluoresce green. Ethidium-homodimer-1 enters dead cells with damaged membranes and undergoes a 40-fold enhancement of fluorescence upon binding to their DNA causing the nuclei of dead cells to fluoresce red. Double-staining cells anchored on the bone graft discs allows simultaneous examination of both live and dead cells on the materials.

A Wst-1 assay was then used to quantify the cell viability [48,49]. Wst-1 measures mitochondrial dehydrogenase activity [50] and refers to 2-(4-iodophenyl)-3-(4-nitrophenyl)-5-(2,4-disulfophenyl)-2H-tetrazolium, monosodium salt (Dojindo, Gaithersburg, MD). At 14 d, specimens with cells were transferred to wells in a 24-well plate and rinsed with 1 ml of Tyrode's Hepes buffer. One milliliter of Tyrode's Hepes buffer and 0.1 ml of Wst-1 solution (5 mmol/l Wst-1 and 0.2 mmol/l 1-methoxy-5-methylphenazinium methylsulfate in water) were added to each well and incubated at 37°C for 2 h. Then 200 μl of each reaction mixture was transferred to a 96-well plate and the absorbance at 450 nm was measured with a microplate reader (Wallac 1420 Victor^2, Perkin Elmer Life Sciences, Gaithersburg, MD).

2.4. Microscopy and statistics

A scanning electron microscope (SEM, JEOL 5300, Peabody, MA) was used to examine the specimens and the cells on the specimens. Cells cultured for 1 d on specimens were rinsed with saline, fixed with 1% volume fraction of glutaraldehyde, subjected to graded alcohol dehydrations, rinsed with hexamethyldisilazane, and then sputter coated with gold.

One standard deviation was used as the estimated standard uncertainty of the measurements. These values should not be compared with data obtained in other laboratories under different conditions. Two- and one-way ANOVA were performed to detect significant effects. Tukey's multiple comparison was used to compare the data at a family confidence coefficient of 0.95.

3. Results

3.1. Effects of chitosan and powder:liquid ratio on mechanical properties

Fig. 1 plots flexural strength and elastic modulus vs. powder:liquid ratio. For strength, two-way ANOVA identified significant effects of powder:liquid ratio and

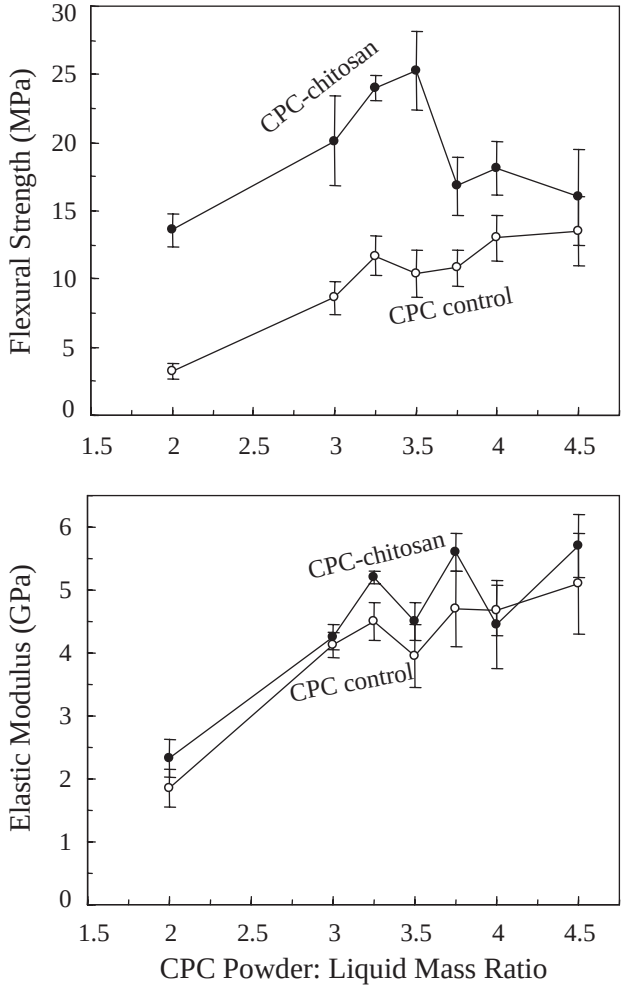

Fig. 1. The incorporation of chitosan significantly increased the strength of CPC–chitosan composite compared to CPC control without chitosan. Modulus increased with powder:liquid ratio, but there is no significant difference between CPC–chitosan and CPC control. The CPC powder is the same for both materials. For CPC control, the liquid is distilled water. For the CPC–chitosan material, the liquid is water plus 15% chitosan. Each value is the mean of six measurements with the error bar showing one standard deviation.

whether chitosan was added or not ($p<0.001$). At each powder:liquid ratio except 4.5, the strength of CPC–chitosan composite was significantly higher than that of CPC control without chitosan ($p<0.001$). The strength of CPC–chitosan was (13.6 ± 1.2) MPa at powder : liquid = 2, significantly higher than (3.2 ± 0.6) MPa for CPC control (Tukey's multiple comparison test; family confidence coefficient = 0.95). At powder: liquid ratio = 3.5, CPC–chitosan had a strength of (25.3 ± 2.9) MPa, significantly higher than (10.4 ± 1.7) MPa for CPC control at the same powder:liquid ratio, and higher than (13.0 ± 1.7) MPa for CPC control at a powder:liquid ratio of 4 (Tukey's at 0.95). At a powder:liquid ratio of 4, the pastes were dry for both materials; at 4.5 ratio, the pastes were very dry and powdery. For elastic modulus, increasing the powder: liquid ratio from 2 to 3 significantly increased the elastic modulus for both materials ($p<0.001$), but there was little difference between the two materials.

3.2. Effect of chitosan on biocompatibility

Cells cultured for 1 d are shown in Fig. 2: (A) live cells on CPC control without chitosan, (B) live cells on CPC–chitosan composite, (C) live cells on TCPS control (tissue culture polystyrene as a biocompatible control), and (D) dead cells on CPC–chitosan. Live cells, stained green, appeared to have adhered and attained a normal polygonal morphology on all materials. Visual examination revealed that the density of live cells adherent to each material was similar. Dead cells (stained red) were very few on all three materials. SEM micrographs in Figs. 3A and B show cell attachment on CPC control and CPC–chitosan composite, respectively. The cells developed cytoplasmic processes with lengths ranging from about 20 to 50 μm that attached to the specimen surfaces. These cytoplasmic extensions are regions of the cell plasma membrane that contain a meshwork or bundles of actin-containing microfilaments which permit the movement of the migrating cells along a substratum [51]. The three materials supported similar cell attachment and development of cytoplasmic processes.

Cells cultured for 14 d are shown in Fig. 4, in which live cells (stained green) had formed a confluent monolayer on all three materials. The 14 d live cell density was much greater than the 1 d density in Fig. 2, indicating that the cells had greatly proliferated. The live cell density appeared similar on the three materials. Again very few dead cells were found. These results suggest that cell proliferation was similar, demonstrating that CPC–chitosan composite was as non-cytotoxic as CPC control and TCPS control. Fig. 4E shows the viability of cells cultured for 2 weeks on CPC–chitosan composite and CPC control, which was quantitatively assessed with the colorimetric Wst-1 assay by measuring the mitochondrial dehydrogenase activity. TCPS was not included since the growth area of the 24-well TCPS plates was larger than the cement discs and hence would not allow an accurate comparison. The Wst-1 assay

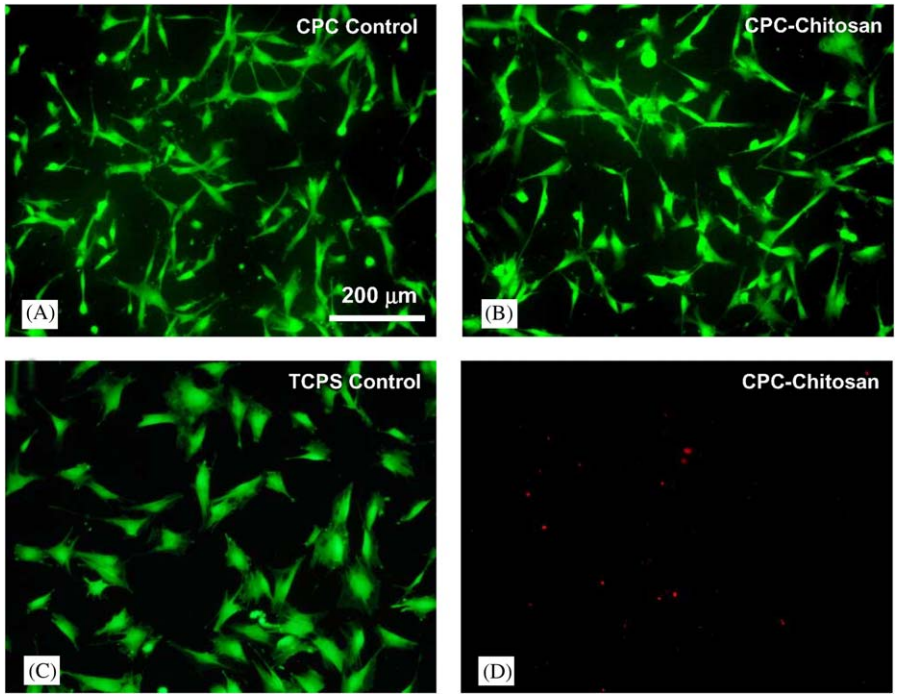

Fig. 2. Cells cultured for 1 d with live cells stained green and dead cells stained red. (A) Live cells on CPC control without chitosan, (B) live cells on CPC–chitosan composite, (C) live cells on TCPS control (tissue culture polystyrene as a biocompatible control), and (D) dead cells on CPC–chitosan.

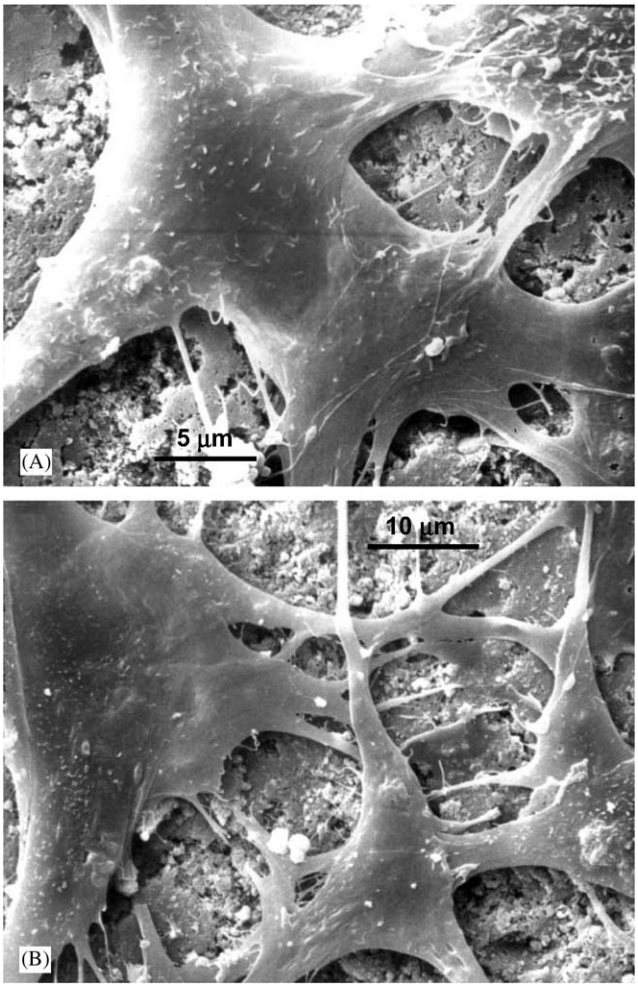

Fig. 3. SEM of cell attachment on (A) CPC control and (B) CPC–chitosan composite. The cells developed cytoplasmic processes with lengths ranging from approximately 20 to 50 μm, and the materials exhibited similar cell attachment and cytoplasmic processes development.

measured the absorbance at 450 nm, which was proportional to the amount of dehydrogenase activity in the cells, to be 0.45 ± 0.10 for CPC control and 0.40 ± 0.09 for CPC–chitosan composite (mean $\pm$ sd; $n = 6$). These two values are statistically similar (Student's t; $p > 0.1$), showing that similar cell dehydrogenase activity was present and hence cell viability was quantitatively similar for CPC–chitosan and CPC control.

3.3. Effect of porosity on scaffold mechanical properties

The specimens in which the mannitol was dissolved were used to measure the density and porosity using Eqs. (1) and (2). The values are reported in Table 1. When the mannitol content was increased from 0% mass fraction to 70%, the CPC–chitosan density (mean $\pm$ sd; $n = 6$) decreased from (1.82 ± 0.02) g/cm^3 to (0.63 ± 0.01) g/cm^3. The total porosity increased from (42.0 ± 0.6)% to (80.0 ± 0.3)%, and the macroporosity reached (65.5 ± 0.8)%. Fig. 5A is an SEM photograph of a typical scaffold with an intermediate mannitol fraction of 50% and hence 57.2% macroporosity. Fig. 5B is a higher magnification showing a well-formed macropore in the shape of the entrapped mannitol crystal. Arrows in Fig. 5C indicate open connections in the bottom of a macropore.

The flexural strength and elastic modulus of these scaffold specimens are plotted in Fig. 6 as a function of macropore volume fraction. At 70% mannitol (Table 1) that yielded a macropore volume fraction of 65.5%, the scaffold had a strength of (0.3 ± 0.1) MPa; this was significantly lower than (0.8 ± 0.2) MPa at 62.6% macroporosity and (1.8 ± 0.2) MPa at 57.2% macroporosity (Tukey's at family confidence coefficient = 0.95). The scaffold strength at 50.4% macroporosity was (1.6 ± 0.2) MPa, significantly lower than (2.4 ± 0.1), (6.8 ± 0.6) and (8.4 ± 0.7) MPa at macroporosities of 41.2%, 29.7% and 17.6%, respectively (Tukey's at 0.95).

The elastic modulus of the scaffold with 65.5% macroporosity was (0.04 ± 0.02) GPa; this was significantly lower than (0.29 ± 0.01) GPa at 62.6% macroporosity and (0.47 ± 0.03) GPa at 57.2% macroporosity (Tukey's at 0.95). The scaffold modulus at 50.4% macroporosity was (0.53 ± 0.13) GPa, significantly lower than (1.00 ± 0.26), (2.19 ± 0.17) and (2.94 ± 0.36) GPa at macroporosities of 41.2%, 29.7% and 17.6%, respectively (Tukey's at 0.95).

3.4. Cells inside pores of scaffold

Cells cultured for 1 and 14 d are shown in Figs. 7A and B, respectively, for a scaffold with an intermediate mannitol mass fraction of 50% that yielded a macroporosity of 57.2%. Significant cell proliferation occurred after 14 d (Fig. 7B). A confluent cell layer was observed on most of the surfaces of the 14-d specimens, but there were spots not covered by a confluent cell layer. Fig. 8A is an SEM showing an example of cell infiltration into a macropore. It appeared that the pore was large enough for the cell, and the cell had completely entered into the pore. Arrows in Fig. 8B indicate cell attachment to the bottom wall of the pore. Fig. 8C shows infiltrated cells near an opening at the bottom of a large pore (similar to the bottom openings in Fig. 5C). Fig. 8D shows cell–cell interactions with the arrow pointing to the formation of a cell–cell junction between two cells inside a pore.

4. Discussion

Highly porous fast-hardening CPC–chitosan scaffold with a total porosity of up to 80% volume fraction, and a macroporosity of up to 65.5% was developed. A major disadvantage of current orthopedic implant materials such as sintered hydroxyapatite is that they exist in a

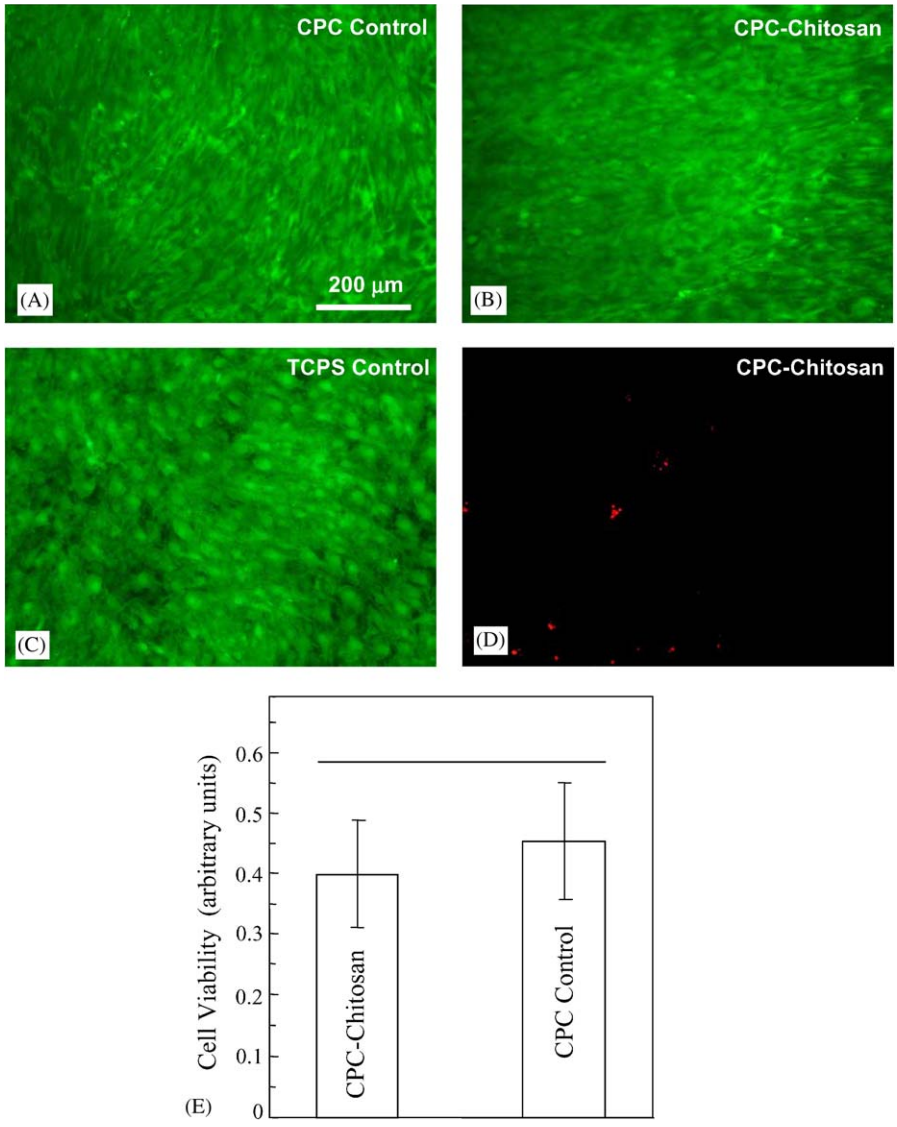

Fig. 4. Cells cultured for 14 d with live cells stained green that had formed a confluent monolayer on all three materials due to cell proliferation. Similar live cell density was observed on the three materials (A–C) with very few dead cells (D). Hence, CPC–chitosan composite was as biocompatible as CPC control and TCPS control. In (E), cell viability was quantified using the colorimetric Wst-1 assay and found to be statistically similar for CPC control and CPC–chitosan composite.

Table 1
Density, macroporosity and total porosity volume fraction of CPC–chitosan scaffolds (mean ± sd; $n = 6$)

Mannitol mass fraction (%) in CPC	CPC–chitosan scaffold density (g/cm^3)	Macroporosity (%)	Total porosity (%)
0	1.82 ± 0.02	0	42.0 ± 0.6
10	1.5 ± 0.02	17.6 ± 2.0	52.2 ± 0.6
20	1.28 ± 0.02	29.7 ± 1.1	59.2 ± 0.6
30	1.07 ± 0.03	41.2 ± 2.2	65.9 ± 1.0
40	0.90 ± 0.03	50.4 ± 1.9	71.2 ± 0.8
50	0.78 ± 0.02	57.2 ± 1.7	75.2 ± 0.7
60	0.68 ± 0.04	62.6 ± 2.7	78.3 ± 1.3
70	0.63 ± 0.01	65.5 ± 0.8	80.0 ± 0.3

hardened form, requiring the surgeon to fit the surgical site around the implant or to carve the graft to the desired shape. This can lead to increases in bone loss, trauma to the surrounding tissue, and longer surgical time [1]. Therefore, the moldability and in situ self-hardening ability of the new scaffolds in the present study make them desirable materials for orthopedic repair. The CPC–mannitol powder can be mixed with the chitosan–water liquid to form a paste that can be applied in surgery via minimally invasive techniques such as injection [14], with fast-setting and anti-washout capabilities [23] to form a highly porous scaffold in situ. Further studies are needed to investigate the effects of

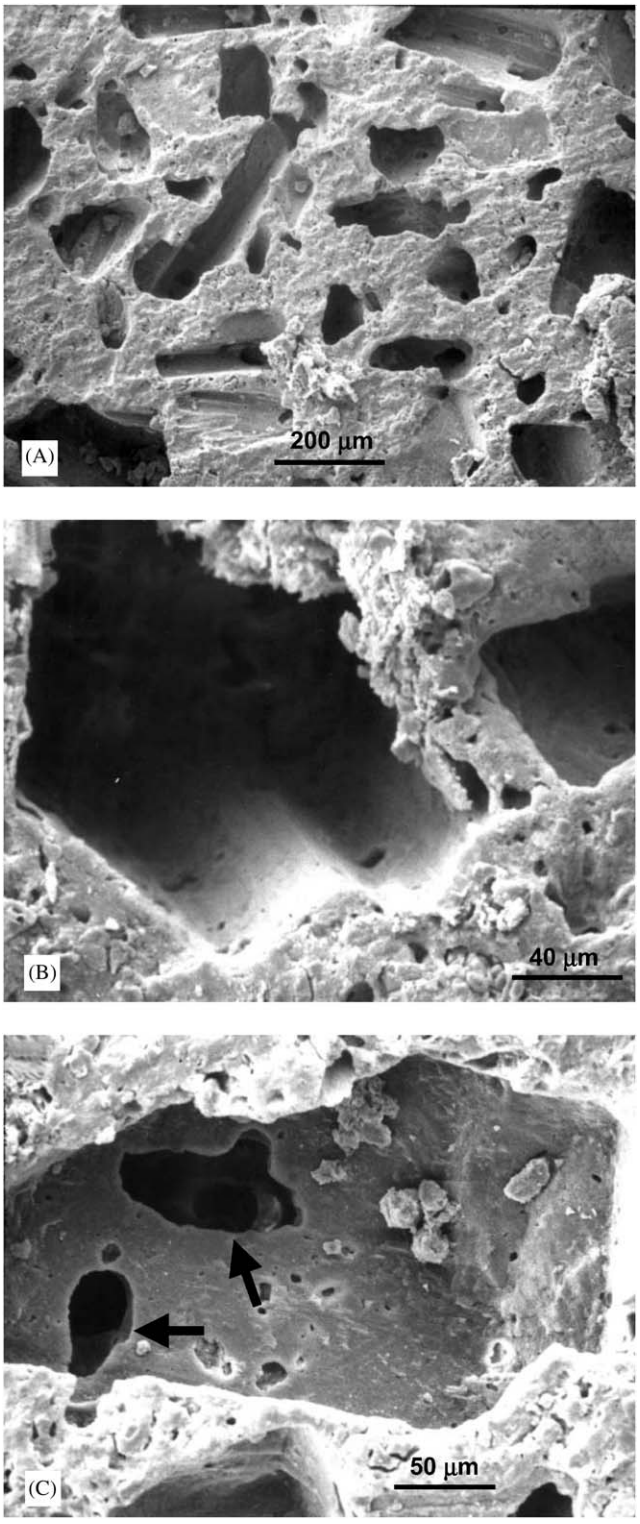

Fig. 5. SEM of CPC–chitosan scaffold with 50% mannitol and 57.2% macropore volume fraction: (A) low magnification; (B) higher magnification of a macropore in the shape of the entrapped mannitol crystal; (C) open connections in the bottom of a macropore (arrows).

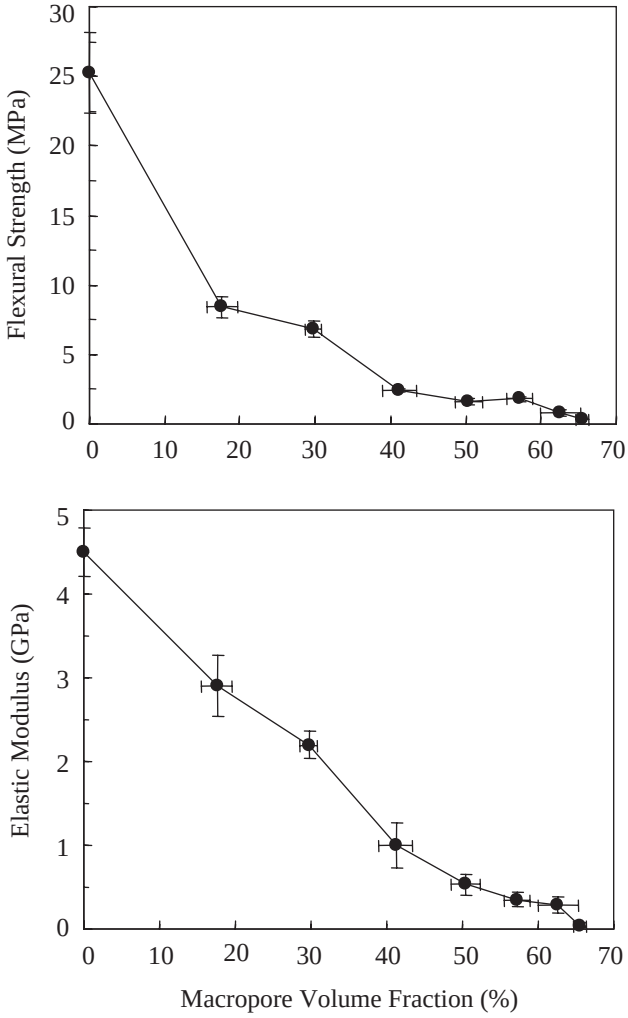

Fig. 6. Flexural strength and elastic modulus vs. macropore volume fraction for CPC–chitosan–mannitol scaffold. The macropores were formed after mannitol dissolution. The porosity values corresponded to mannitol fractions in Table 1. Each value is mean ± sd, $n = 6$.

mannitol content and powder-to-liquid ratio on the injectability of the paste.

Substantial increases in strength over the conventional CPC were achieved for the CPC–chitosan composite. At powder:liquid ratios of 3 and 3.5, the strength was increased by about three times due to chitosan incorporation (Fig. 1); at powder:liquid ratio = 2, the strength was increased by 4.3 times. When the mannitol was dissolved to form the scaffolds, the implant strength was 6.8 MPa at a macropore volume fraction of about 30%; the strength then became 1.8 MPa at 57% macroporosity. In comparison, the flexural strength of sintered porous hydroxyapatite implants ranges from 2 to 11 MPa [3]. Compared to sintered hydroxyapatite, the new CPC–chitosan scaffold is advantageous because it can harden in situ without machining. With a macroporosity of 41–57%, and a total porosity of 65.9–75.2%, the CPC–chitosan scaffold had strength values close to the strength of about 3.5 MPa for cancellous bone [52]. The elastic modulus of cancellous bone ranged from 50 to 300 MPa [53]. These values are also similar to the modulus of the

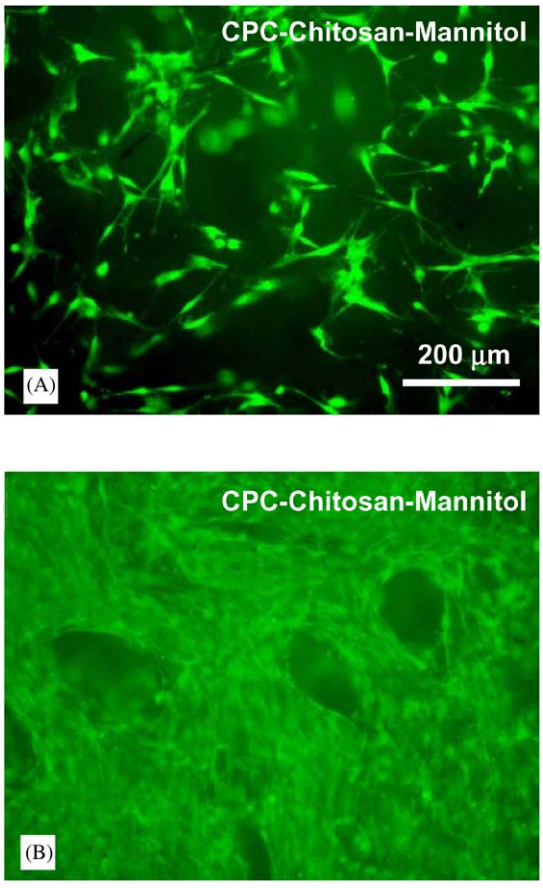

Fig. 7. (A) and (B) Cells cultured for 1 and 14 d, respectively, for scaffold with 57.2% macroporosity. Significant cell proliferation occurred in 14 d.

CPC–chitosan scaffold at total porosity ranging from 71.2% to 80.0%.

In a previous study on the development of fast-setting CPC scaffolds [23], a CPC–chitosan–mannitol composite was examined that contained a single mannitol/(mannitol + CPC powder) mass fraction of 50%, with 15% of chitosan in the liquid. Flexural strength of this composite was measured to be 1.2 MPa after 1 d immersion [23]. In the present study, the CPC with the same 15% chitosan and the same 50% mannitol (resulting in a macroporosity of 57.2%) had a higher flexural strength of 1.8 MPa after 1 d immersion. This is likely because in the previous study a powder:liquid ratio of 3 was used [23], while in the present study a more optimum powder:liquid ratio of 3.5 was used which resulted in a higher strength than that at a ratio of 3 (Fig. 1). Regarding the effect of immersion time on properties, the previous study [23] measured the flexural strength of CPC–chitosan-mannitol scaffold at immersion times from 1 to 84 d. The flexural strength decreased from 1.2 MPa at 1 d to 0.8 MPa at 84 d immersion, a drop of 33% over a period of 3 months. Previous studies showed that significant bone ingrowth into porous implants occurred in several weeks [26,54], and normal bone remodeling and healing took a period over a few months [25,55]. Bone ingrowth was observed to significantly increase the strength of the macroporous implants [24,56]. Therefore, the mild strength decrease over 3 months for the CPC–chitosan–mannitol scaffold should provide time for bone ingrowth into the scaffold to strengthen the implant and avoid a too rapid strength loss.

Regarding the macropore size in the scaffold, a previous study measured the size distribution of the same batch of mannitol crystals used in the present study. The mannitol particles had a diameter of (165 ± 44) μm and a length of (271 ± 72) μm [23]. Pore sizes of this range were shown to be suitable for cell infiltration and bone ingrowth in previous studies [25,26,28,57]. Previous studies showed that sintered hydroxyapatite implants had pore volume fractions from about 40% to 48% and as high as 75% [25,26]. These values corresponded to macroporosities of 29.7–65.5% for the new CPC–chitosan scaffold. One advantage of the CPC–chitosan scaffold over sintered hydroxyapatite is that, while sintered hydroxyapatite is more stable in vivo, CPC can be resorbed and replaced by new bone [15–19]. Therefore, the pore sizes and pore volume fractions of the CPC scaffold are expected to increase over time in vivo.

The porosities in this self-hardening scaffold should enhance the bone ingrowth and implant fixation. Animal studies are needed to investigate the implant fixation and more rapid bone formation as a function of macropore volume fraction for these new scaffolds. Another potential advantage of the high porosity of the new CPC–chitosan scaffold may be the increased bioresorption of the implant due to the increased porosity. Animal studies showed that the conventional CPC was slowly resorbed and replaced by new bone [15]. One study on alveolar ridge augmentation observed CPC resorption at 6 months after surgery [57]. Another study showed little resorption of CPC or formation of new bone at 6 months in vivo [15]. After 9–18 months, about half of the CPC implant was resorbed and replaced by new bone [15,17]. It is desirable to shorten the resorption time of CPC in vivo to a few weeks or a few months. This is because previous studies showed that significant bone ingrowth into porous implants occurred in a few weeks [54,26], and normal bone remodeling and healing took a period of a few months [55,25]. Creating a high macroporosity in CPC increases the graft surface area and may help shorten its resorption time. While our ongoing preliminary animal studies showed faster resorption and new bone formation for the new CPC–chitosan-mannitol scaffold as compared to the conventional CPC, more systematic studies are needed to establish the resorption rate of CPC over a wide range of macropore volume fractions.

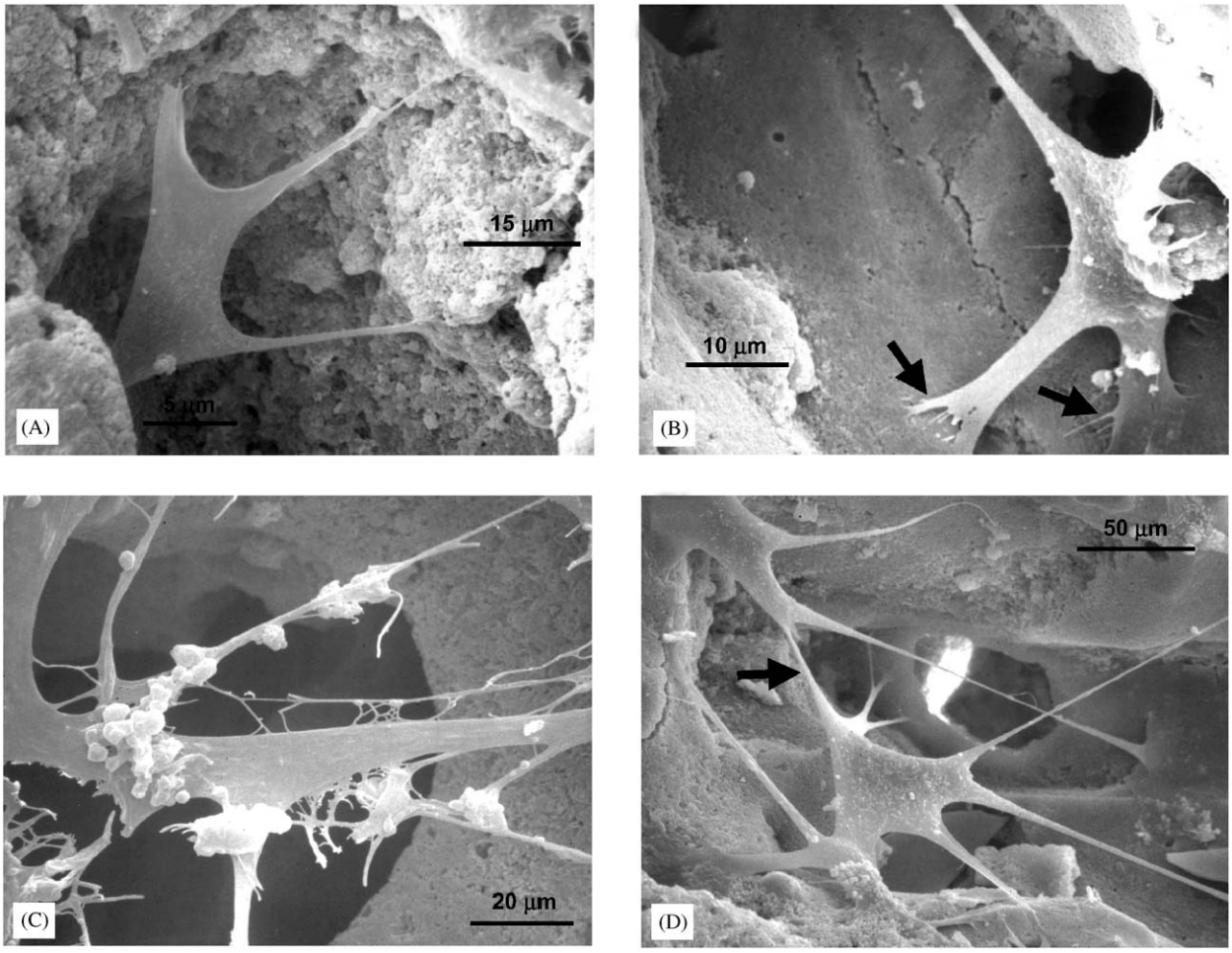

Fig. 8. (A) SEM of cell infiltration into a macropore. (B) Cell attachment (arrows) to the bottom of a pore. (C) Cells inside a large pore near an opening at the bottom of the pore. (D) Cell–cell interactions inside a pore (arrow indicates a cell–cell junction).

The present study showed that the CPC–chitosan scaffold bone graft was biocompatible. After 1 d cell culture, the osteoblast mouse cells (MC3T3-E1) were able to adhere, spread and remain viable on CPC–chitosan composite, CPC control and TCPS when observed by fluorescence microscopy. After 14 d cultures, fluorescence microscopy and the quantitative Wst-1 assay showed that cell adhesion, proliferation and viability were equivalent on these materials. Therefore, these in vitro cell culture results suggest that the new CPC–chitosan composite was non-cytotoxic. Cells were able to adhere and attain a normal morphology on CPC–chitosan-mannitol scaffold specimens; however, proliferation appeared to be slower on these specimens. It is possible that mannitol may have interacted with cell proliferation, but this would require further experimentation to determine. The cells appeared to be able to infiltrate into the macropores of the CPC–chitosan-mannitol scaffold because the pore sizes (165–271 μm [23]) were much larger than the size of the cells ranging from about 20 to 50 μm including the cytoplasmic extensions. Cell attachment and cell–cell interactions were established inside the pores of the scaffold. Further studies should try to quantify the cell secretion of extracellular matrix components in the scaffold in bioreactors.

5. Summary

This study imparted substantial reinforcement and macroporosity to a moldable, self-hardening and resorbable hydroxyapatite cement. The flexural strength of the new CPC–chitosan composite was three to four times higher than the conventional CPC. A powder-to-liquid mass ratio of 3.5 resulted in the highest strength for the CPC–chitosan composite. The scaffold possessed a total pore volume fraction from 42.0% to 80.0%, and a macroporosity up to 65.5%. At total porosities of 52.2–75.2%, the scaffold had strength and elastic modulus values similar to those of sintered porous hydroxyapatite and cancellous bone. The new CPC–chitosan formulation was biocompatible and supported the adhesion, spreading, proliferation and viability of

osteoblast cells. The cells were observed to infiltrate into the pores of the scaffold and establish cell–cell interactions. The increased strength and macroporosity of the new apatite scaffold may help facilitate bone ingrowth, implant fixation, and more rapid new bone formation. The fast-setting (hardening in 8.2 min [23]), anti-washout scaffold paste of the present study could be directly applied to fit complex shapes of bone defects, without involving machining as in the case of sintered hydroxyapatite. The synergistic use of a reinforcing agent (e.g., chitosan) and a pore-forming agent (e.g., mannitol) in a bone graft may be applicable to other tissue engineering materials.

Acknowledgements

We thank Drs. F.C. Eichmiller and N.R. Washburn for discussions, and A.A. Giuseppetti and L.E. Carey for experimental assistance. This study was supported by USPHS Grants DE12476 and DE14190, NIST, and the ADAF.

Disclaimer

Certain commercial materials and equipment are identified in this paper to specify experimental procedures. In no instance does such identification imply recommendation by NIST or the ADA Foundation or that the material identified is necessarily the best available for the purpose.

References

[1] Laurencin CT, Ambrosio AMA, Borden MD, Cooper Jr JA. Tissue engineering: orthopedic applications. Annu Rev Biomed Eng 1999;1:19–46.

[2] LeGeros RZ, LeGeros JP. Dense hydroxyapatite. In: Hench LL, Wilson J, editors. An introduction to bioceramics. New Jersey: World Scientific; 1993. p. 139–80.

[3] Suchanek W, Yoshimura M. Processing and properties of hydroxyapatite-based biomaterials for use as hard tissue replacement implants. J Mater Res 1998;13:94–117.

[4] Brown WE, Chow LC. A new calcium phosphate water setting cement. In:Brown PW, editor. Cements research progress. Westerville, OH: American Ceramic Society; 1986. p. 352–79.

[5] Ginebra MP, Fernandez E, De Maeyer EAP, Verbeeck RMH, Boltong MG, Ginebra J, Driessens FCM, Planell JA. Setting reaction and hardening of an apatite calcium phosphate cement. J Dent Res 1997;76:905–12.

[6] Constantz BR, Barr BM, Ison IC, Fulmer MT, Baker J, McKinney L, Goodman SB, Gunasekaren S, Delaney DC, Ross J, Poser RD. Histological, chemical, and crystallographic analysis of four calcium phosphate cements in different rabbit osseous sites. J Biomed Mater Res (Appl Biomater) 1998;43:451–61.

[7] Knaack D, Goad MEP, Aiolova M, Rey C, Tofighi A, Chakravarthy P, Lee DD. Resorbable calcium phosphate bone substitute. J Biomed Mater Res (Appl Biomater) 1998;43:399–409.

[8] Miyamoto Y, Ishikawa K, Takechi M, Toh T, Yuasa T, Nagayama M, Suzuki K. Histological and compositional evaluations of three types of calcium phosphate cements when implanted in subcutaneous tissue immediately after mixing. J Biomed Mater Res (Appl Biomater) 1999;48:36–42.

[9] Barralet JE, Gaunt T, Wright AJ, Gibson IR, Knowles JC. Effect of porosity reduction by compaction on compressive strength and microstructure of calcium phosphate cement. J Biomed Mater Res (Appl Biomater) 2002;63:1–9.

[10] Yokoyama A, Yamamoto S, Kawasaki T, Kohgo T, Nakasu M. Development of calcium phosphate cement using chitosan and citric acid for bone substitute materials. Biomaterials 2002;23:1091–101.

[11] Gisep A, Wieling R, Bohner M, Matter S, Schneider E, Rahn B. Resorption patterns of calcium-phosphate cements in bone. J Biomed Mater Res 2003;66A:532–40.

[12] Ehara A, Ogata K, Imazato S, Ebisu S, Nakano T, Umakoshi Y. Effects of α-TCP and TetCP on MC3T3-E1 proliferation, differentiation and mineralization. Biomaterials 2003;24:831–6.

[13] Yuasa T, Miyamoto Y, Ishikawa K, Takechi M, Momota Y, Tatehara S, Nagayama M. Effects of apatite cements on proliferation and differentiation of human osteoblasts in vitro. Biomaterials 2004;25:1159–66.

[14] Apelt D, Theiss F, El-Warrak AO, Zlinszky K, Bettschart-Wolfisberger R, Bohner M, Matter S, Auer JA, von Rechenberg B. In vivo behavior of three different injectable hydraulic calcium phosphate cements. Biomaterials 2004;25:1439–51.

[15] Friedman CD, Costantino PD, Jones K, Chow LC, Pelzer HJ, Sisson GA. Hydroxyapatite cement: II, obliteration and reconstruction of the cat frontal sinus. Arch Otolaryngol Head Neck Surg 1991;117:385–9.

[16] Costantino PD, Friedman CD, Jones K, Chow LC, Sisson GA. Experimental hydroxyapatite cement cranioplasty. Plast Reconstr Surg 1992;90:174–91.

[17] Shindo ML, Contantino PD, Friedman CD, Chow LC. Facial skeletal augmentation using hydroxyapatite cement. Arch Otolaryngol Head Neck Surg 1993;119:185–90.

[18] Friedman CD, Costantino PD, Takagi S, Chow LC. BoneSource™ hydroxyapatite cement: a novel biomaterial for craniofacial skeletal tissue engineering and reconstruction. J Biomed Mater Res (Appl Biomater) 1998;43:428–32.

[19] Chow LC. Calcium phosphate cements: chemistry, properties, and applications. Mater Res Symp Proc 2000;599:27–37.

[20] Ishikawa K, Miyamoto Y, Takechi M, Toh T, Kon M, Nagayama M, Asaoka K. Non-decay type fast-setting calcium phosphate cement: hydroxyapatite putty containing an increased amount of sodium alginate. J Biomed Mater Res 1997;36:393–9.

[21] Xu HHK, Quinn JB, Takagi S, Chow LC. Processing and properties of strong and non-rigid calcium phosphate cement. J Dent Res 2002;81:219–24.

[22] Takagi S, Chow LC, Hirayama S, Eichmiller FC. Properties of elastomeric calcium phosphate cement-chitosan composites. Dent Mater 2003;797–804.

[23] Xu HHK, Takagi S, Quinn JB, Chow LC. Fast-setting calcium phosphate scaffolds with tailored macropore formation rates for bone regeneration. J Biomed Mater Res 2004;68A:725–34.

[24] Shors EC, Holmes RE. Porous hydroxyapatite. In: Hench LL, Wilson J, editors. An introduction to bioceramics. New Jersey: World Scientific; 1993. p. 181–98.

[25] Pilliar RM, Filiaggi MJ, Wells JD, Grynpas MD, Kandel RA. Porous calcium polyphosphate scaffolds for bone substitute applications—in vitro characterization. Biomaterials 2001;22:963–72.

[26] Tamai N, Myoui A, Tomita T, Nakase T, Tanaka J, Ochi T, Yoshikawa H. Novel hydroxyapatite ceramics with an inter-

connective porous structure exhibit superior osteoconduction in vivo. J Biomed Mater Res 2002;59:110–7.
[27] Chu TMG, Orton DG, Hollister SJ, Feinberg SE, Halloran JW. Mechanical and in vivo performance of hydroxyapatite implants with controlled architectures. Biomaterials 2002;23:1283–93.
[28] Tsuruga E, Takita H, Itoh H, Wakisaka Y, Kuboki Y. Pore size of porous hydroxyapatite as the cell-substratum controls BMP-induced osteogenesis. J Biochem 1997;121:317–24.
[29] Hing KA, Best SM, Bonfield W. Characterization of porous hydroxyapatite. J Mater Sci Mater Med 1999;10:135–45.
[30] Damien E, Hing K, Saeed S, Revell PA. A preliminary study on the enhancement of the osteointegration of a novel synthetic hydroxyapatite scaffold in vivo. J Biomed Mater Res 2003; 66A:241–6.
[31] Roy TD, Simon JL, Ricci JL, Rekow ED, Thompson VP, Parsons JR. Performance of hydroxyapatite bone repair scaffolds created via three-dimensional fabrication techniques. J Biomed Mater Res 2003;67A:1228–37.
[32] Ishaug SL, Crane GM, Miller MJ, Yasko AW, Yaszemski MJ, Mikos AG. Bone formation by three-dimensional stromal osteoblast culture in biodegradable polymer scaffolds. J Biomed Mater Res 1997;36:17–28.
[33] Langer R, Vacanti JP. Tissue engineering. Science 1993;260:920–6.
[34] Livingston T, Ducheyne P, Garino J. In vivo evaluation of a bioactive scaffold for bone tissue engineering. J Biomed Mater Res 2002;62:1–13.
[35] Ma PX, Zhang R, Xiao G, Franceschi R. Engineering new bone tissue in vitro on highly porous poly(α-hydroxyl acids)/hydroxyapatite composite scaffolds. J Biomed Mater Res 2001;54: 284–93.
[36] Murphy WL, Kohn DH, Mooney DJ. Growth of continuous bonelike mineral within porous poly(lactide-co-glycolide) scaffolds in vitro. J Biomed Mater Res 2000;50:50–8.
[37] Brown GD, Mealey BL, Nummikoski PV, Bifano SL, Waldrop TC. Hydroxyapatite cement implant for regeneration of periodontal osseous defects in humans. J Periodontol 1998;69:146–57.
[38] Takagi S, Chow LC. Formation of macropores in calcium phosphate cement implants. J Mater Sci Mater Med 2001;12: 135–9.
[39] Xu HHK, Quinn JB, Takagi S, Chow LC, Eichmiller FC. Strong and macroporous calcium phosphate cement: effects of porosity and fiber reinforcement on mechanical properties. J Biomed Mater Res 2001;57:457–66.
[40] Xu HHK, Quinn JB. Calcium phosphate cement containing resorbable fibers for short-term reinforcement and macroporosity. Biomaterials 2002;23:193–202.
[41] Xu HHK, Quinn JB, Takagi S, Chow LC. Synergistic reinforcement of in situ hardening calcium phosphate composite scaffold for bone tissue engineering. Biomaterials 2004;25:1029–37.
[42] Machida Y, Nagai T, Abe M, Sannan T. Use of chitosan and hydroxypropyl chitosan in drug formulations to effect sustained release. Drug Dis Deliv 1986;1:119–30.
[43] Muzzarelli RAA, Biagini G, Bellardini M, Simonelli L, Castaldini C, Fraatto G. Osteoconduction exerted by methylpyrolidinone chitosan in dental surgery. Biomaterials 1993;14:39–43.
[44] Muzzarelli RAA. Amphoteric derivatives of chitosan, their biological significance. In: Skjak-Brak G, Anthonsen T, Sandford P, editors. Chitin and chitosan. New York: Elsevier Applied Science; 1989. p. 87–99.
[45] Xu HHK, Eichmiller FC, Giuseppetti AA. Reinforcement of a self-setting calcium phosphate cement with different fibers. J Biomed Mater Res 2000;52:107–14.
[46] International Standards Organization. ISO 10993-5. Biological evaluation of medical devices — part 5: tests for in vitro cytotoxicity. International Standards Organization; Geneva, Switzerland; 1999.
[47] Attawia MA, Uhrich KE, Botchwey E, Langer R, Laurencin CT. In vitro bone biocompatibility of poly(anhydride-co-imides) containing pyromellitylimidoalanine. J Orthopaed Res 1996;14:445–54.
[48] Simon Jr CG, Khatri CA, Wight SA, Wang FW. Preliminary report on the biocompatibility of a moldable, resorbable, composite bone graft consisting of calcium phosphate cement and poly(lactide-co-glycolide) microspheres. J Orthop Res 2002; 20:473–82.
[49] Xu HHK, Smith DT, Simon Jr CG. Strong and bioactive composites containing nano-silica-fused whiskers for bone repair. Biomaterials 2004;25:4615–26.
[50] Ishiyama M, Shiga M, Sasamoto K, Mizoguchi M, He P-g. A new sulfonated tetrazolium salt that produces a highly water-soluble formazan dye. Chem Pharm Bull 1993;41:1118–22.
[51] Darnell J, Lodish H, Baltimore D. Molecular cell biology, 2nd ed. New York: Freeman and Company; 1990. p. 890–91.
[52] Damien CJ, Parsons JR. Bone graft and bone graft substitutes: a review of current technology and applications. J Appl Biomater 1991;2:187–208.
[53] O'Kelly K, Tancred D, McCormack B, Carr A. A quantitative technique for comparing synthetic porous hydroxyapatite structure and cancellous bone. J Mater Sci Mater Med 1996;7:207–13.
[54] Chang BS, Lee CK, Hong KS, Youn HJ, Ryu HS, Chung SS, Park KW. Osteoconduction at porous hydroxyapatite with various pore configurations. Biomaterials 2000;21:1291–8.
[55] Shikinami Y, Okuno M. Bioresorbable devices made of forged composites hydroxyapatite (HA) particles and poly-L-lactide (PLLA): part I. Basic characteristics. Biomaterials 1999;20: 859–77.
[56] Martin RB, Chapman MW, Holmes RE, Sartoris DJ, Shors EC, Gordon JE, Heitter DO, Sharkey NA, Zissimos AG. Effects of bone ingrowth on the strength and non-invasive assessment of a coralline hydroxyapatite material. Biomaterials 1989;10:481–8.
[57] Sugawara A, Fujikawa K, Kusama K, Nishiyama M, Murai S, Takagi S, Chow LC. Histopathologic reaction of a calcium phosphate cement for alveolar ridge augmentation. J Biomed Mater Res 2002;61:47–52.